Biomaterials 33 (2012) 8822–8829

Contents lists available at SciVerse ScienceDirect

Biomaterials

journal homepage: www.elsevier.com/locate/biomaterials

Riboflavin carrier protein-targeted fluorescent USPIO for the assessment of vascular metabolism in tumors

Jabadurai Jayapaul [a,b], Susanne Arns [a], Wiltrud Lederle [a], Twan Lammers [a], Peter Comba [b], Jessica Gätjens [a], Fabian Kiessling [a,*]

[a] Department of Experimental Molecular Imaging, RWTH Aachen University, Pauwelsstrasse 30, 52074 Aachen, Germany
[b] Anorganisch-Chemisches Institut, Universität Heidelberg, Im Neuenheimer Feld 270, 69120 Heidelberg, Germany

ARTICLE INFO

Article history:
Received 19 June 2012
Accepted 16 August 2012
Available online 6 September 2012

Keywords:
Endothelium
Flavin adenine dinucleotide
Iron oxide nanoparticles
Magnetic resonance imaging
Molecular imaging
Riboflavin carrier protein

ABSTRACT

Riboflavin (Rf) and its metabolic analogs flavin mononucleotide (FMN) and flavin adenine dinucleotide (FAD) are essential for normal cellular growth and function. Their intracellular transport is regulated by the riboflavin carrier protein (RCP), which has been shown to be over-expressed by metabolically active cancer cells. Therefore, FAD-decorated ultrasmall superparamagnetic iron oxide nanoparticles (FAD USPIO) were developed as the first carrier-protein-targeted molecular MR agents for visualizing tumor metabolism. FAD USPIO were synthesized using an adsorptive, fluorescent and non-polymeric coating method, and their physicochemical properties were characterized using TEM, SEM, FTIR, MRI and fluorescence spectroscopy. *In vitro* analyses showed the biocompatibility of FAD USPIO, and confirmed that they were strongly and specifically taken up by cancer (LnCap) and endothelial (HUVEC) cells. *In vivo* molecular MRI together with subsequent histological validation finally demonstrated that FAD USPIO efficiently accumulate in tumors and tumor blood vessels, indicating that RCP-targeted diagnostic nanoparticles are interesting new materials for the assessment of vascular metabolism in tumors.

1. Introduction

Flavin adenine dinucleotide (FAD), a metabolic analog of riboflavin (Rf), is a cofactor of different redox enzymes and mediates the energy metabolism in mitochondria [1,2]. It acts as the principal electron acceptor moiety in combination with the electron donor counterpart NADH (nicotinamide adenine dinucleotide) to regulate cellular metabolism [3]. The oxidation-reduction ratio of the NADH/FAD redox systems is significantly increased in cancer cells as compared to normal cells [4] thus illustrating its high cellular metabolism [5]. The transport of Rf and its metabolic co-factors like flavin mononucleotide (FMN) into cells is facilitated by a phosphoglycoprotein expressed on the surface of cellular membranes, namely riboflavin carrier protein (RCP) [6]. Endogenous FAD possesses a hydrophobic isoalloxazine ring and a hydrophilic ribityl side chain similar to FMN and Rf, which are responsible for its strong binding affinity to RCP and thus mediate its active transport into cells (receptor-mediated endocytosis) [7,8]. The regulation of RCP expression is believed to be high in cells with elevated metabolic activity (e.g. tumor cells) [9] and in activated endothelial cells. In line with this, RCP is also up-regulated in different prostate cancer cells (PC-3, DU-145 and LnCap) [10]. Therefore, RCP might serve as an attractive biomarker for tumor metabolism and as an interesting target for molecular targeted diagnostic and therapeutic agents. The fact that RCP-mediated uptake can be clathrin-based [11] further helps to rapidly transport larger molecules (e.g. diagnostic nanoparticles, drug-loaded polymers, dendrimers, liposomes) into cells [12–16]. In this context, we recently demonstrated that adsorptively FMN-coated ultrasmall superparamagnetic iron oxide nanoparticles (FLUSPIO) can be efficiently used for RCP-mediated targeting of different prostate cancer and activated endothelial cells *in vitro* [17]. Here, we present a flavin-based ligand system as an adsorptive coating molecule for iron oxide nanoparticles, which is anticipated to display enhanced binding affinity for RCP and to promote high intracellular accumulation of the tagged diagnostics. In addition, for the first time, successful RCP-mediated molecular MR imaging of angiogenic vessels in tumors is shown *in vivo*.

The search for relevant flavin-based ligand systems lead us to the vitamin B2 analog FAD, which is endogenous, fluorescent and exhibits strong interaction for RCP. Intending to develop RCP-targeted molecular MRI contrast agents, FAD was considered to

* Corresponding author.
E-mail address: fkiessling@ukaachen.de (F. Kiessling).

0142-9612/$ – see front matter © 2012 Elsevier Ltd. All rights reserved.
http://dx.doi.org/10.1016/j.biomaterials.2012.08.036

be a promising candidate for adsorptive coating of iron oxide nanoparticles, due to the predictable binding via two phosphate groups. The amine group of the adenosine moiety of FAD would then be available for further functionalization with biomolecules (e.g. peptides, antibodies etc.). We hypothesize that this molecular MR probe will display better pharmacokinetics, increased stability without agglomeration under physiological conditions, due to the presence of pyrophosphate groups (for stronger binding to nanoparticles) that link nucleoside adenosine, which amplifies glucose signaling during metabolism [18] to the Rf moiety.

After the chemical and physical characterization of the FAD-decorated ultrasmall superparamagnetic iron oxide nanoparticles (FAD USPIO), its potential as a molecular MR contrast agent was evaluated both *in vitro and in vivo*. In this context, FAD USPIO nanoparticles were investigated for their efficiency in MR cell labeling and their specificity for RCP was evaluated *in vitro* by competitively blocking RCP. Furthermore, the *in vivo* uptake of FAD USPIO mediated by RCP in angiogenic vessels, was studied in prostate cancer xenografts and evident MR findings were co-validated through histology and Prussian blue staining.

2. Experimental

2.1. Materials

Ferric chloride ($FeCl_3$, >97%), ferrous chloride tetrahydrate ($FeCl_2.4H_2O$ >99%), Trypan blue solution for microscopy, IDRANAL III standard solution ((EDTA-Na_2), reagent for metal titration, 0.1 M), 5-sulfosalicylic acid dehydrate (≥99%), potassium bromide (spectroscopic grade) were purchased from Sigma–Aldrich (Steinheim, Germany). Ammonia (≥25%), N-(2-Hydroxyethyl)piperazine-N′-(2-ethanesulfonic acid) (HEPES, ≥99.5%), hydrochloric acid (37%), ammonium peroxodisulfate (≥98%), sodium acetate (≥99%) were obtained from Carl Roth (Karlsruhe, Germany). Guanosine-5′-monophosphate disodium salt hydrate (GMP, 98%), Riboflavin-5′-adenosine disphosphate disodium salt dehydrate (Flavin adenine dinucleotide, FAD, 95–98% analytical grade), Potassium hexacyanoferrate (II) trihydrate (biochemical grade), gelatin (ph. Eur, powder), PBS buffer (10× Dulbecco's powder) were acquired from AppliChem (Darmstadt, Germany). 4′,6-diamidino-2-phenylindole (DAPI) was procured from Merck KGaA, Darmstadt, Germany. Resovist® 0.5 mmol Fe/mL injection solution (carboxydextran-coated iron oxide nanoparticles with a core size of ~4 nm and a mean hydrodynamic size of ~60 nm) was obtained from Bayer Schering AG, Berlin, Germany. All chemicals were used without further purification.

2.2. Synthesis of iron oxide nanoparticles (Fe_3O_4)

Ultrasmall Superparamagnetic Iron Oxide nanoparticles (USPIO) were synthesized by co-precipitation of ferrous (Fe^{2+}) and ferric (Fe^{3+}) salts under aqueous alkaline conditions. A modified one-pot synthesis protocol was followed [19]. A stoichiometric ratio of $2Fe^{3+}$:Fe^{2+}, 16 mmol (2.66 g) of $FeCl_3$ and 8 mmol (1.63 g) of $FeCl_2.4H_2O$, was dissolved in 190 mL de-ionized water. Subsequently, under vigorous stirring, 10 mL of 25% NH_3 was used to prepare magnetite as black precipitate. After 20 min stirring, the particles were washed thrice with water and two times with 0.1 M HCl solution aided by magnetic separation. Then, magnetic fluids were dispersed in 100 mL of 0.1 M HCl. The USPIO were sonicated for 20 min prior to centrifugation at 20,000 *g* for 15 min. The total iron concentration of as-synthesized USPIO determined by titrimetry [20] and colorimetry (tiron method) [21] was 161 mM. A colorimetric method was used additionally to support the results from titrimetry.

2.3. Synthesis of FAD USPIO nanoparticles

We used fluorescent flavin adenine dinucleotide (FAD) and guanosine monophosphate (GMP) as adsorptive coating molecules for USPIO. The non-polymeric coating was achieved by sonication (Ultrasonic cleaner, 30 W, VWR GmbH, Germany) of 143 mM USPIO with 35 mM FAD for 1 h at ambient temperature. Excess uncoated FAD was removed by high-gradient magnetophoresis. Subsequently, FAD-modified particles were sonicated with 50 mM GMP for another 1 h at ambient temperature. Excess of free GMP was removed by high-gradient magnetophoresis to yield the final fluorescent FAD USPIO nanoparticles.

2.4. General characterization – transmission electron microscopy (TEM)

The morphology, size, and size distribution of the nanoparticles were characterized by TEM EM 400 T (Philips, Eindhoven, The Netherlands). USPIO and FAD USPIO were embedded in 2% agarose, rinsed with distilled water and dehydrated with ethanol (30–100%). Subsequently, they were embedded in Epon, polymerized 8 h at 37 °C, 56 h at 60 °C, and then cut into 70–100 nm thick slices. The particle size and size distributions were calculated by measuring the diameter of at least 100 particles using an image analysis program (iTEM software, Olympus, Germany).

2.4.1. Scanning electron microscopy (SEM)

The surface morphology of the nanoparticles was characterized by SEM [FEI (PHILIPS) ESEM XL 30 FEG; EDAX Falcon genesis]. USPIO and FAD USPIO in water were dehydrated as described above. Finally, trace amounts of water was removed by treating them with propylene oxide. Further, samples were dried and mounted on specimen stub with silver paste or graphite prior to SEM measurement.

2.4.2. X-ray powder diffraction (XRD)

The crystal structures of USPIO and FAD USPIO particles were characterized by using the powder diffractometer STOE STADI P equipped with an IP-PSD detector and Cu$K\alpha_1$ as the radiation source (1.54059 Å; STOE & Cie, Darmstadt, Germany).

2.4.3. MR relaxometry (phantom studies)

MR relaxometry of FAD USPIO nanoparticles was performed using a clinical (3T) whole-body MR scanner (Philips Achieva, The Netherlands) in combination with a knee coil (SENSE-flex-M, Philips, The Netherlands) at RT. FAD USPIO and Resovist (clinical SPIO contrast agent) were diluted in de-ionized water at concentrations of 0.005–50 μg Fe/0.3 mL. For MR measurements 0.3 mL of diluted FAD USPIO/Resovist solution was filled in custom made phantoms. For phantom T_2 relaxometry, images at 20 echo times (TE range = 8–180 ms) were acquired by using a multi-slice, multi-shot spin-echo sequence (1500 ms TR, 8.1 ms inter-echo spacing, 96 × 96 reconstruction matrix size, 2 × 2 mm^2 voxel size, 3 mm slice thickness, 130 × 162.5 mm^2 field of view, 90° flip angle). Signal amplitudes were averaged by manually defining regions of interests (ROI); T_2 relaxation times were calculated by a linear fit of the logarithmic signal amplitudes vs. echo time.

T1 maps were acquired by using a multi-slice, multi-shot fast-field-echo Look-Locker inversion recovery sequence using simulated ECG triggering (30 bpm stimulated heart rate, 70 ms phase interval, 6–8 ms TR, 3–4 ms TE, 160 × 160 reconstruction matrix size, 5 mm slice thickness, 170 × 150 mm^2 field of view, 10° flip angle). Further, relaxation signal amplitudes were fitted to a signal model to yield T1 relaxation times. Relaxivities r1 and r2 for FAD USPIO/Resovist were determined by a linear fit of the inverse relaxation times as a function of the iron concentrations.

2.5. Cell culture

LnCap cells were cultured using RPMI medium with glutamax (Gibco, Invitrogen, Germany), supplemented with 20% fetal calf serum (Invitrogen, Germany) and 1% Pen/strep (10,000 U/mL penicillin; 10,000 μg/mL streptomycin, Invitrogen, Germany). HUVEC were cultured using endothelial cell growth medium (Vasculife, Germany) supplemented with endothelial cell growth factors and 1% Pen/Strep. Cells were cultured in T75 cell culture flasks (Cell star, Greiner, Germany) and incubated at 37 °C, 5% CO_2 and 95% relative humidity.

2.5.1. Trypan blue staining

The toxicity of the FAD USPIO on prostate cancer cells (LnCap) was investigated using trypan blue (Sigma–Aldrich, Steinheim, Germany) staining. LnCap cells (2×10^6) were seeded in 6-well plates (BD Falcon, Germany) and incubated overnight. Cells incubated with cell growth medium served as negative controls. The amount of coating molecules (FAD and GMP in μmol/mL) used for controls was concentrated according to their surface concentration on FAD USPIO. FAD USPIO and USPIO were diluted in LnCap cell growth medium to 0.03, 0.3, 3.0 μmol Fe/mL. 1 mL of nanoparticle- or coating molecule-containing medium was added to each well. Triplicates were used per condition. Cells were incubated for 3 h and 24 h. After the incubation, the medium was removed and cells were washed, trypsinized (0.25% trypsin/0.05% EDTA) and centrifuged. The cell pellet was dissolved in 0.5 mL of fresh cell growth medium, stained with trypan blue solution and counted using a Cedex XS (Innovatis AG, Germany) cell counter. The percentage of trypan blue positive cells (dead cells) as a function of the total cell number was calculated. Additionally, the effect of excess Rf (10- and 100-fold), used for competition experiments on LnCap's viability was investigated using trypan blue staining.

2.5.2. Competitive binding experiments with MRI

Competitive binding experiments were performed in order to validate the RCP-mediated uptake of FAD USPIO by metabolically active prostate cancer cells (LnCap). Cells were pre-incubated for 10 min with 10-(Rf) and 100-fold excess (Rf and FAD) with respect to c(FAD) on FAD USPIO. Subsequently, FAD USPIO were added (0.3 μmol Fe/mL) and cells were incubated for 1 h at 37 °C (5% CO_2 and 95% relative humidity). Three samples per condition were analyzed. After incubation, cells were washed with PBS and trypsinized using 4 mL of trypsin/EDTA (0.25%/0.05%). Trypsinization was ceased by adding respective cell growth medium and the cell suspension was centrifuged at 1000 rpm (Multifuge, Thermo scientific, Germany) for 5 min. The cell pellet obtained was re-suspended in 50 mL of PBS buffer and washed thrice by centrifugation. The total cell numbers were counted (2×10^6 cells/0.3 mL) prior to their suspension in 10% gelatin. MR relaxometry of cells was performed at

the clinical 3T MRI (Philips) scanner using the MR-sequences as described under phantom studies section.

Furthermore, the uptake of FAD USPIO by HUVEC was compared to that by LnCap cells. Both cell types were incubated with USPIO and FAD USPIO (0.03, 0.3 μmol Fe/mL) for 1 h. Cells were washed, trypsinized, centrifuged and suspended in 10% gelatin as discussed above, prior to the MR-evaluation.

2.6. Inhibition of cellular FAD USPIO uptake using excess Rf/FAD (fluorescence microscopy analysis)

LnCap cells ($0.5–1.0 \times 10^6$) were seeded on microscopic slides (76 × 26 mm), placed inside the quadriPERM chamber (Greiner, Germany) and incubated for 24 h with regular growth medium. Subsequently, cells were washed with PBS buffer and pre-incubated (10 min) with free flavin (10- and 100-fold Rf (FAD precursor); 100-fold FAD) and then incubated for 1 h with FAD USPIO (0.3 μmol Fe/mL) in the growth medium. Other cell samples were incubated with control USPIO for 1 h. After the incubation, the cells were washed thrice with PBS and fixed using 4% paraformaldehyde (PFA). Cell nuclei were stained with DAPI. Cover slips were mounted on the microscopic slides using mowiol mounting medium prior to the microscopic (ImagerM2, Carl Zeiss Microimaging GmbH, Germany) evaluation. Triplicates were used for all conditions.

2.7. In vivo uptake of FAD USPIO by LnCap xenografts (MRI)

All animal experiments were approved by the governmental review committee on animal care. Eight CD1 male nude mice (Charles River Laboratories International, Inc., Wilmington, MA, USA) with human prostate cancer (LnCap) tumors were used for the *in vivo* evaluation (uptake studies) of FAD USPIO ($n = 4$) and of Resovist ($n = 4$). LnCap tumor xenografts were induced by subcutaneous injection of 4×10^6 LnCap cells [22] into the right hind limb of the mice. MR investigations were carried out after the tumors had reached a size of 4 × 4 mm^2 (volume of 33 mm^3). The nude mice bearing LnCap tumors were injected intravenously with FAD USPIO or Resovist (control) at the dosage of 900 μmol Fe/Kg. MR imaging of LnCap tumor xenografts pre- and post-particle injection (1 h and 3 h) under isoflurane anesthesia was performed using a clinical 3T MRI system, in combination with a custom-made small animal solenoid sense-receive mouse coil (40 mm inner diameter and 78 mm bore length, resulting in a 40-mm field of view)(Philips Research Laboratories, Hamburg, Germany), and the head-to-tail symmetry line was placed perpendicular to B_0 in the magnet bore.

To visualize anatomic details, transverse high-spatial resolution T_2-weighted MR images of the tumors were acquired by using a multi-shot turbo-spin-echo sequence with the following parameters: 1400 ms/100 ms (TR/TE), 0.2 × 0.2 mm^2 voxel size, 1 mm slice thickness, 144 × 144 reconstruction matrix size and 25 mm field of view. For *in vivo* T_2^* relaxometry, images at 15 echo times (TE range = 10–190 ms) were acquired by using a multi-shot, multi-slice fast-field-echo sequence (125 ms TR, 7.9 ms interval between two echoes, 144 × 144 reconstruction matrix size, 0.3 × 0.3 mm^2 voxel size, 1 mm slice thickness, 40 mm field of view, 30° flip angle).

For *in vivo* T_2^*-weighted MR images, the same location was measured with fast-field-echo sequences (117 ms TR, 26 ms TE, 96 × 96 reconstruction matrix size, 0.2 × 0.2 mm^2 voxel size, 1 mm slice thickness, 25 mm field of view, 30° flip angle).

An interactive display language (IDL, version 6.1) implementation of the above algorithms was applied for post-processing on the basis of PAR/REC4 images. Further, color-coded R_2^* relaxation rate pixel maps of tumors (FAD USPIO/Control) were generated using the "PRIDE" analysis software (Philips Healthcare).

2.8. Prussian blue staining

Prussian blue staining was performed to visualize the accumulation of Resovist and FAD USPIO inside the LnCap prostate tumors and muscle tissue. The tumors/muscles were cryo-preserved (−80 °C) and covered with tissue tek (O.C.T. Compound, Sakura Finetek Europe B.V., Germany). For the Prussian blue stain, 8 μm thin sections of the tumor/muscle tissues were prepared using a cryotom (Leica GmbH, Germany). Tumor and muscle sections were first incubated (5 min) with an aqueous solution of $K_4Fe(CN)_6$ (10%), followed by a 1:1 mixture of $K_4Fe(CN)_6$ (10%) and HCl acid (20%) for 30 min. Subsequently, sections were counterstained (10 min) with Nuclear Fast Red (Carl Roth, Karlsruhe, Germany). After staining, the sections were washed with water, dried with ethanol, rinsed with xylene, mounted using *in vitro* clud (R. Langenbrinck GmbH, Germany) and prepared for the microscopic analysis (Imager M2, Carl Zeiss Microimaging GmbH, Germany).

2.9. Immunohistochemistry of LnCap tumors and muscle

The LnCap tumor and muscle sections (8 μm) on microscopic slides (76 × 26 mm) were stained for vascularization using a primary rat anti-mouse CD31 (PECAM-1) endothelial cell marker antibody (Dianova GmbH, Hamburg, Germany) for 2 h (RT) in association with a Cy3-labeled anti-rat IgG secondary antibody (Dianova GmbH, Hamburg, Germany), for 40 min (RT), respectively. Nuclei were counterstained with DAPI. Cover slips were mounted on LnCap tumor and muscle sections using mowiol mounting medium. The microscopic slides were analyzed by fluorescence microscopy (Imager M2, Carl Zeiss GmbH, Germany) at different magnifications (10×, 20× and 40×) and fields of view.

3. Results and discussion

3.1. FAD USPIO characterization

USPIO nanoparticles, prepared by co-precipitation, were coated with non-polymeric, fluorescent FAD, which strongly binds to the iron oxide cores via pyrophosphate groups (Fig. 1A). The FAD coating was achieved in aqueous solution, with reaction conditions analogous to the FLUSPIO synthesis at pH 4, by sonication at ambient temperature [17]. Excess uncoated ligand (FAD) was removed by employing high-gradient magnetophoresis. The initial fluorescent coating of USPIO with FAD alone lead to particle agglomeration (visual inspection), which could be attributed to the equilibrium between the open and stacked configuration of the dimethyl isoalloxazine ring with the adenosine moiety of FAD in solution. Additionally, to sustain the FAD fluorescence without quenching, the equilibrium shift toward a stacked FAD configuration (prone to quenching) was prevented by partial coverage of the nanoparticles surface. The loss in stability due to partial surface coverage of FAD USPIO was minimized by introducing the less bulky and smaller guanosine monophosphate (GMP), such that the remaining surface of USPIO was covered completely during the non-polymeric coating. The inherent negative charge of GMP and FAD promotes their binding to positively charged USPIO cores at low pH and confers an overall negative surface charge to the nanoparticles and fostering its colloidal stability under physiological conditions. The free amine available in the guanine moiety of GMP similar to FAD also provides an opportunity to tag biomolecules with nanoparticles using standard conjugation techniques, thereby promoting molecular MR imaging.

Transmission electron microscopy (TEM), nanoparticle tracking analysis (NTA) and scanning electron microscopy (SEM) were used to characterize the FAD USPIO. The TEM analysis of USPIO and FAD USPIO showed nanoparticles with an average iron core size of 5.84 ± 1.03 nm and 5.83 ± 1.05 nm, respectively (Table 1 and Fig. 1B). SEM was used to study the surface morphology of the nanoparticles and revealed a spherical morphology of the particles, with an average particle size of 23.89 ± 5.38 nm for USPIO and 26.52 ± 4.83 nm for FAD USPIO (Fig. 1C). The increase in size (by SEM) of FAD USPIO compared to USPIO is presumably due to strong assembly of nanoparticles upon drying or due to a conductive (thick) layer of sputtered gold on the nanoparticle surface. The NTA analysis showed particles with size distributions of 93.00 ± 7.94 nm for USPIO and 118.66 ± 5.51 nm for FAD USPIO (both suspended in 5% glucose solution, which was also used in the *in vivo* experiments). In line with this, the photographs of FAD USPIO dispersed in cell growth media (RPMI, McCoy's) enriched with FCS (fetal calf serum), different solutions (water, 5% glucose solution) and HEPES buffer, display stability of the suspension for over 180 min without visible sedimentation (Fig. 1E). USPIO showed similar results in 5% glucose solution but sedimented within 15 min in HEPES buffer possibly due to propagation of large agglomerates of iron cores at increasing pH (Fig. 1D).

Zeta potential measurements were performed to determine the surface charge, electrophoretic mobility and colloidal stability of the USPIO and FAD USPIO particles at pH 2, 7 and 9 (Table 1). Under low and neutral pH conditions USPIO had a positive zeta potential, presumably owing to their highly protonated surfaces. Furthermore, under basic conditions USPIO displayed a negative zeta potential possibly due to the deprotonation of surface groups (terminal or bridging OH), respectively. FAD USPIO displayed a negative zeta potential under physiological conditions, which is

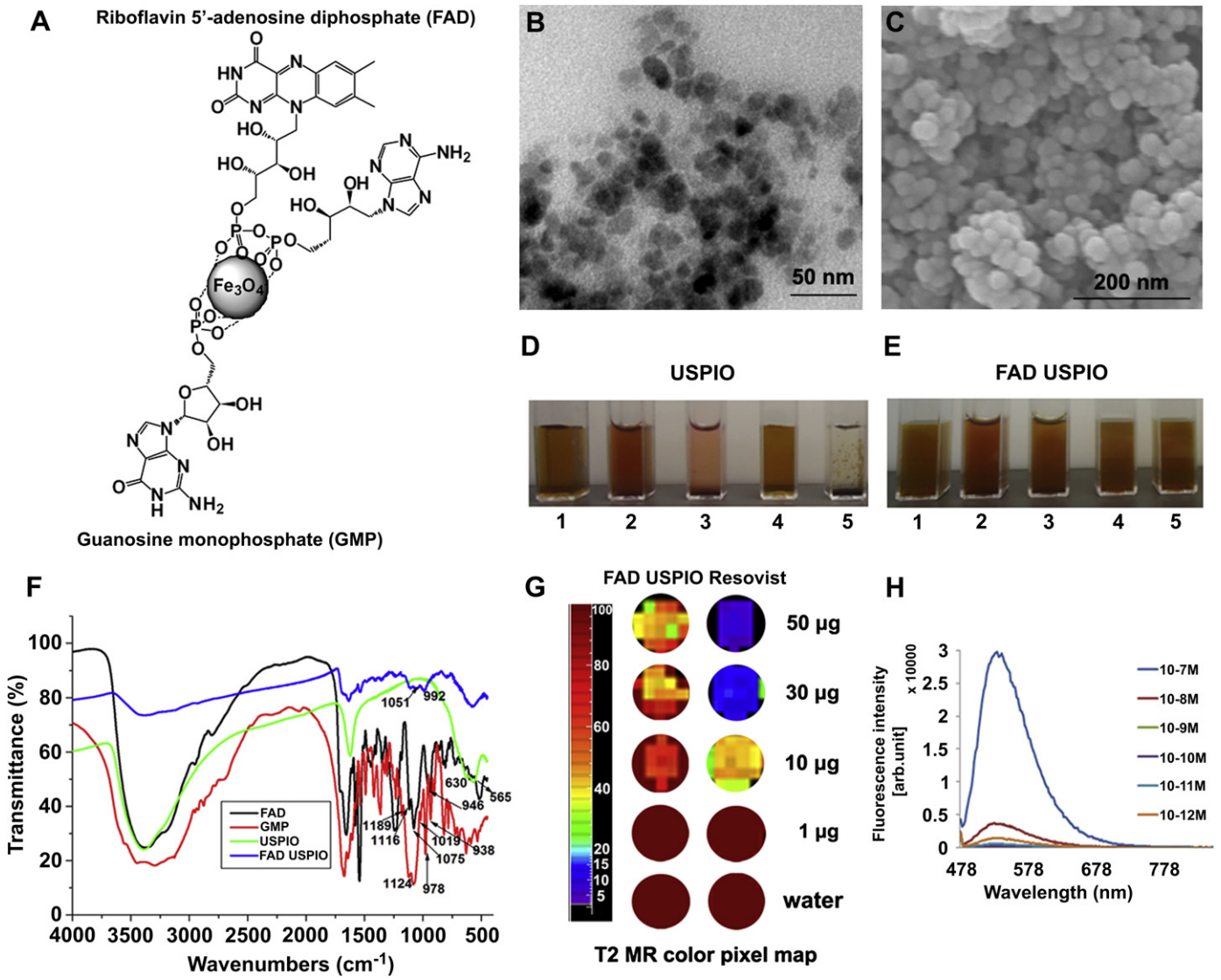

Fig. 1. Preparation and physico-chemical characterization of FAD USPIO. A: Schematic diagram showing the adsorptive interaction of FAD and GMP with the iron oxide nanoparticles. B: TEM and C: SEM images of FAD USPIO. Quantitative analysis of these images reveals a core size of 5.83 ± 1.05 nm (by TEM) and an average diameter of 26.52 ± 4.83 nm (by SEM), respectively. D, E: Photographs of USPIO and FAD USPIO dispersed in different physiological solutions (1: water, 2: McCoy's and 3: RPMI cell culture media enriched with FCS, 4: 5% glucose solution, 5: 25 mM HEPES buffer). FAD USPIO are stable in solutions (1–5) for 3 h without agglomeration, whereas USPIO displayed sedimentation in solutions 3 and 5. F: FT-IR spectra of FAD USPIO compared to controls (FAD, GMP, USPIO) supported that the binding of FAD/GMP to iron oxide nanoparticles occurs via (pyro-)phosphate groups. G, H: Evaluation of FAD USPIO's magnetic and fluorescent properties in water: color-coded T_2 relaxation time pixel maps of FAD USPIO and of Resovist in de-ionized water indicate that there is a comparable dose-dependent decrease in signal intensity (G). FAD USPIO shows an intense emission at 530 nm due to the high payload of FAD on the surface of iron oxide nanoparticles (H).

highly beneficial for its pharmacokinetic behavior *in vivo*. Under acidic conditions, FAD USPIO had a positive zeta potential, as anticipated, due to prominent protonation of the ensemble of nanoparticles. Furthermore, FAD USPIO had a negative zeta potential under basic conditions, which can be explained by the intrinsic negative charge of the coating molecules (FAD, GMP) and by the high payload of anions at basic pH-values.

Table 1
Physico-chemical characterization of USPIO and FAD USPIO.

Samples	TEM size (nm)	Zeta potential (mV)		
		pH 2	pH 7	pH 9
USPIO	5.84 ± 1.03	27.03 ± 3.74	33.80 ± 5.02	−27.36 ± 1.14
FAD USPIO	5.83 ± 1.05	24.50 ± 1.61	−27.96 ± 0.11	−25.83 ± 2.06

X-ray powder diffraction (XRD) analysis was used to determine the chemical composition and crystallinity of USPIO and FAD USPIO. The observed diffraction patterns of USPIO are in line with the anticipated diffraction reflections of Fe_3O_4 (Supporting Information, Figure S1). The XRD patterns of FAD USPIO are attributed to (220), (311), (400) reflections, arising from spinel structure of magnetite (JCPDS No. 19-0629). Fourier-transform infrared spectroscopy (FT-IR) supported the binding of FAD and GMP to iron oxide nanoparticles via the pyrophosphate and phosphate groups, which was validated by analyzing free FAD, GMP and unmodified USPIO (Fig. 1F). The chemical composition of the FAD USPIO surface (concentration of FAD, GMP) was analyzed by energy-dispersive X-ray (EDX) spectroscopy, Vaskovsky phosphate determination, elemental analysis and thermo-gravimetric analysis (TGA) (Supporting Information). The observed Fe:P ratio for the fluorescent nanoparticles determined by EDX (1:0.145) was

in close agreement with the theoretically calculated ratio of phosphorous to iron. Furthermore, the results on the chemical composition of FAD USPIO were supported by the Vaskovsky phosphate determination (Table S1 in the "Supporting Information") and elemental analysis. TGA of the FAD USPIO showed a weight loss of 26% when heated to 600 °C (Supporting Information, Figure S2). This clearly accounts for the decomposition of the adsorptive surface coating (FAD and GMP) and for the dehydration of the USPIO's inorganic matrix (theoretically calculated weight loss: 27%).

3.2. Magnetic and fluorescent properties of FAD USPIO

The MR relaxivity of the FAD USPIO in de-ionized water at 3T (RT) was found to be similar to that of the clinical MR contrast agent ferucarbotran (Resovist®, Bayer Schering AG, Berlin, Germany) (FAD USPIO: $r2 = 84.70 \pm 1.57\ s^{-1}\ mM^{-1}$, $r1 = 1.53 \pm 1.56\ s^{-1}\ mM^{-1}$; Resovist: $r2 = 132.90 \pm 0.29\ s^{-1}\ mM^{-1}$, $r1 = 3.23 \pm 1.37\ s^{-1}\ mM^{-1}$; Fig. 1G), thereby indicating a potential usefulness as MR contrast agent. Fluorescence spectroscopy of the FAD USPIO revealed a high fluorescence intensity due to the high loading of the FAD fluorophore, associated with the metallic nanoparticle surface [23]. The fluorescent nanoparticles (FAD USPIO) can be excited in a wide wavelength range (350–500 nm), resulting in an intense emission at 530 nm (Fig. 1H and Supporting Information, Figure S3).

3.3. Cytotoxicity of FAD USPIO

The viablility of LnCap (human prostate cancer) cells labeled with FAD USPIO or being exposed to 10- and 100-fold Rf was investigated using trypan blue stain. As shown in the supporting information, Figure S4, trypan blue staining indicated no significant change in cell viability at FAD USPIO concentrations, which are suited for cell labeling (i.e. up to 0.3 μmol Fe/mL). Also the addition of Rf did not lead to decreased cell viability up to a concentration of 30 μmol/mL.

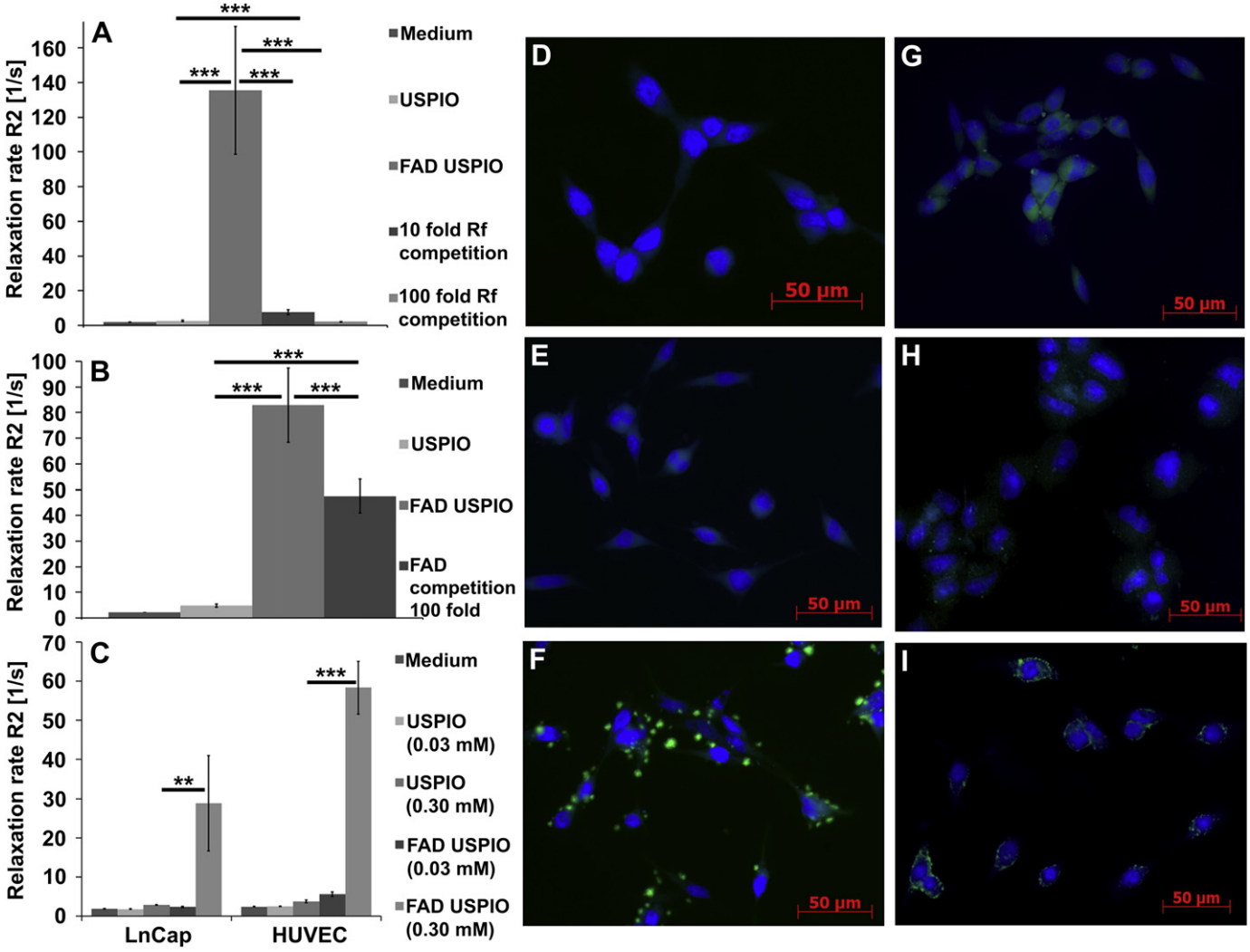

Fig. 2. Cellular uptake and specificity of FAD USPIO for RCP investigated by MRI and fluorescence microscopy. A,B: R_2 relaxation rates of LnCap cells in gelatin (2.0×10^6 cells/0.3 mL) incubated (1 h) with 0.3 μmol Fe/mL of USPIO, FAD USPIO, FAD USPIO plus free Rf (10- and 100-fold excess)(A) and FAD USPIO plus free FAD (100-fold excess for competition purposes)(B). C: R_2 relaxation rates of LnCap cells and HUVEC (2×10^6 cells/0.3 mL in gelatin) incubated with 0.3 and 0.03 μmol Fe/mL of USPIO, FAD USPIO for 1 h. In all cases, a two-tailed unpaired student *t*-test was used to test for statistical significance ***: $p < 0.001$; **: $p < 0.005$. D–F: Fluorescence microscopy images of LnCap cells incubated for 1 h with FAD USPIO (0.3 μmol Fe/mL). Nuclei are counterstained with DAPI. D: Blank medium. E: USPIO. F: FAD USPIO plus DAPI. The microscopy images clearly show vesicular localization of the FAD USPIO, indicating endosomal uptake. G,H: The uptake of FAD USPIO (0.3 μmol Fe/mL) by LnCap cells after 1 h was competitively inhibited by the addition of free Rf (10- and 100-fold excess) and by 100-fold FAD addition, respectively (I). Together, these results confirm the RCP-mediated specific uptake of FAD USPIO by LnCap cells.

3.4. Cellular labeling and competition (MRI and fluorescence microscopy)

Subsequently, the cellular labeling efficiency and the uptake of FAD USPIO by metabolically active prostate cancer (LnCap) and activated human umbilical vein endothelial (HUVEC) cells were investigated by MRI (3T). LnCap cells are known to express high RCP-levels [10], and thus were chosen to evaluate the RCP-mediated specific uptake of FAD USPIO. Additionally, as a model of activated endothelial cells, the uptake of FAD USPIO by HUVEC was studied hypothesizing that an activated angiogenic endothelium will have elevated RCP-levels due to its increased metabolism. In this context, the cells were labeled with FAD USPIO, re-suspended in 10% gelatin (2×10^6 cells/0.3 mL; 0.3 μmol Fe/mL, 1 h) and the R_2 relaxation rates were determined. Each condition used for cell labeling was performed in triplicates. LnCap cells in gelatin showed a significantly higher R_2 relaxation rate after 1 h incubation with FAD USPIO ($135.56 \pm 36.78\ s^{-1}$, $p < 0.001$) than USPIO ($2.76 \pm 0.43\ s^{-1}$) indicating a higher cellular uptake of FAD USPIO. As it is known from literature that RCP interacts and binds specifically with flavins (Rf, FMN and FAD) in different ratios [24], it should be possible to competitively block the RCP-mediated specific uptake of FAD USPIO by the addition of free flavins to the growth medium. After the addition of free Rf to LnCap cells and subsequent incubation with FAD USPIO for 1 h, the R_2 relaxation rates were significantly reduced (10-fold Rf competition: $7.76 \pm 1.42\ s^{-1}$, $p < 0.001$; 100-fold Rf competition: $2.22 \pm 0.15\ s^{-1}$, $p < 0.001$; vs. FAD USPIO incubation alone: $135.56 \pm 36.78\ s^{-1}$)(Fig. 2A).

In line with these results the specific uptake of FAD USPIO by LnCap cells was also competitively inhibited using free FAD (100-fold). Again, LnCap cells incubated with FAD USPIO displayed a significantly higher R_2 relaxation rate ($82.93 \pm 14.49\ s^{-1}$) after 1 h incubation compared to cells under competition conditions (100-fold FAD: $47.48 \pm 6.57\ s^{-1}$, $p < 0.001$)(Fig. 2B). The high cellular uptake of FAD USPIO by LnCap cells was further confirmed using fluorescence microscopy (Fig. 2D–I). A strong green fluorescence in the cells was observed after FAD USPIO incubation (1 h) (Fig. 2F). The perinuclear fluorescence pattern strongly suggests endosomal uptake of FAD USPIO. Additionally, competitively inhibiting FAD USPIO uptake by free Rf (10- and 100-fold excess), and by 100-fold FAD, resulted in a strong reduction of green fluorescence inside cells (Fig. 2G–I). Together, these results indicate that there is a strong RCP-mediated uptake of FAD USPIO into the endosomes of LnCap cells.

In addition to RCP-overexpressing prostate cancer cells, we also investigated the uptake of FAD USPIO in HUVEC as a model for activated endothelium. Surprisingly, HUVEC incubated for 1 h with FAD USPIO (0.3 μmol Fe/mL), showed a significantly higher R_2 relaxation rate ($58.34 \pm 6.74\ s^{-1}$, $p < 0.001$) than LnCap cells ($28.83 \pm 12.18\ s^{-1}$, $p < 0.005$) and HUVEC incubated with USPIO alone ($3.74 \pm 0.35\ s^{-1}$), respectively (Fig. 2C).

The *in vitro* results indicate that imaging RCP-expression may provide a promising new biomarker to assess increased cellular metabolism *in vivo*. Its evaluation for cancer diagnosis is reasonable since ^{18}FDG (fluoro-2-deoxy-D-glucose), the most extensively used molecular diagnostic agent for cancer diagnosis in the clinic, also characterizes a metabolic pathway. However, since nanoparticles are used in this approach, which are known to only extravasate in small amounts and thus will hardly reach tumor cells *in vivo* [25], we expected a predominant labeling of the activated endothelial cell compartment and thus providing indirect information about vascular activation and angiogenesis.

3.5. In vivo uptake of FAD USPIO

The RCP-mediated *in vivo* uptake of FAD USPIO and its anticipated ability as an angiogenic vessel marker was evaluated using CD1 male nude mice bearing LnCap tumors ($n = 4$). Animals ($n = 4$) treated with Resovist served as a control. Resovist® are carboxydextran-coated iron oxide nanoparticles with a core size of 4.2 nm, a hydrodynamic size of ~60 nm and a zeta potential of -34.36 ± 2.30 mV (at pH 7). These were used in clinics for macrophage-mediated targeted imaging of the reticuloendothelial system (RES) [26]. There was a significantly stronger increase in R_2^* relaxation rates in tumors 1 h and 3 h after intravenous injection of FAD USPIO, compared to Resovist® (FAD USPIO vs. Resovist® at 1 h: $18.75 \pm 6.96\ s^{-1}$ vs. $5.92 \pm 2.48\ s^{-1}$; $13.66 \pm 4.05\ s^{-1}$ vs. $4.56 \pm 4.91\ s^{-1}$ at 3 h) (Fig. 3G). These changes in R_2^* relaxation rate can also be clearly seen in the color-coded R_2^* maps overlaid on T_2^*-weighted images (Fig. 3A–F). The higher tumor uptake of FAD USPIO in comparison with Resovist® indicates that their

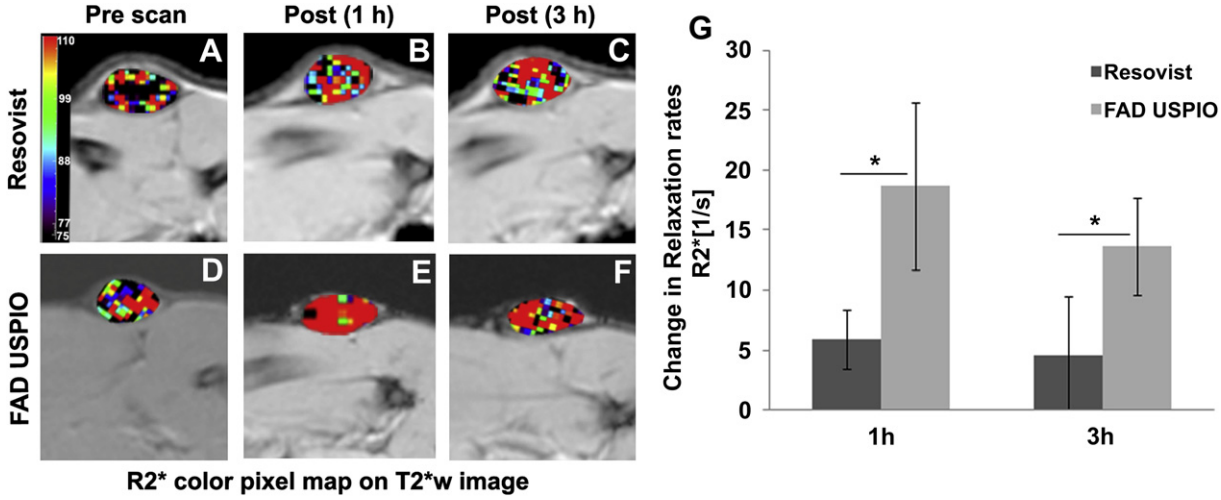

Fig. 3. MRI study on the uptake of FAD USPIO into prostate cancer xenografts. A–F: The R_2^* color-coded pixel maps were overlaid on T_2^*-weighted MR images (transversal slice) of CD1 male nude mice bearing subcutaneous LnCap tumors ($n = 4$) pre and post intravenous injection (1 h and 3 h) of Resovist (A–C) and FAD USPIO (D–F), respectively. The increase in R_2^* relaxation rate 1 h after injection of FAD USPIO can be visualized by an increase of red color in the color pixel map in (E–F) and (G). Much less effect is observed in the control tumor after intravenous injection of Resovist (B–C) and (G). Statistical significance was tested using two-tailed student *t*-test *: $p < 0.05$. (For interpretation of the references to colour in this figure legend, the reader is referred to the web version of this article.)

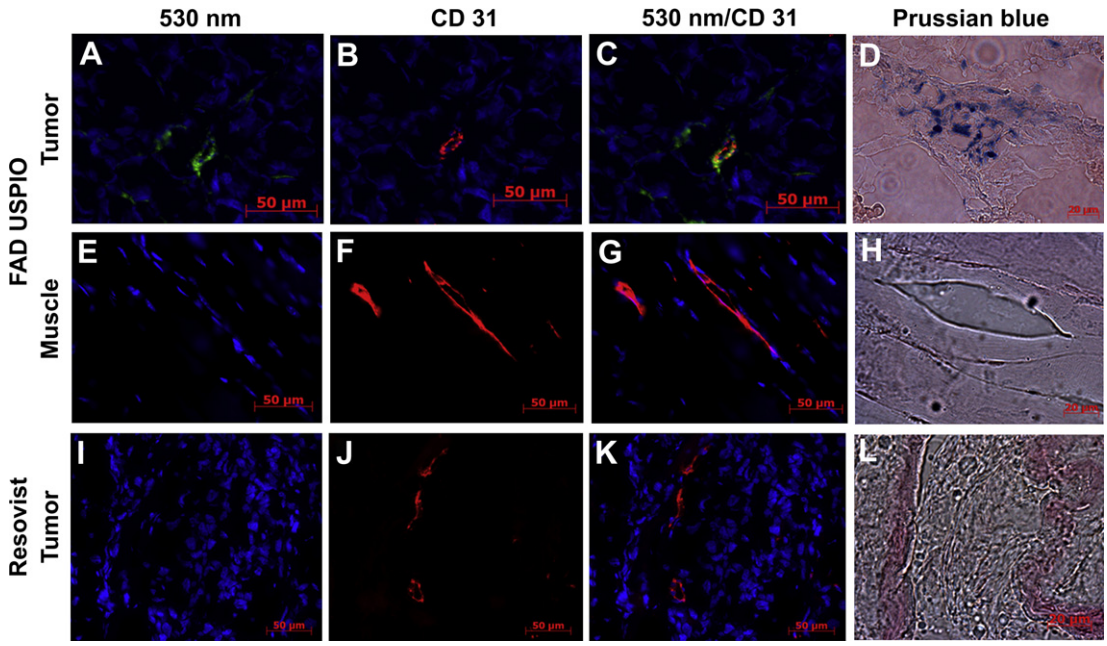

Fig. 4. Histological validation of FAD USPIO accumulation in LnCap tumors. Triple immunofluorescence and Prussian blue stained images of LnCap tumors after injection of FAD USPIO (A–D) and Resovist (I–L). Muscle sections after injection of FAD USPIO are shown in E–H. Tumor vessels were stained using a CD31antibody (red) and nuclei were counterstained with DAPI (blue). FAD USPIO can be visualized at 530 nm. Triple fluorescence-based histological analysis showed highly vascularized tumors with FAD USPIO (green in A) co-localized (yellow in C) inside endothelial cells (red in B). This observation is supported by the Prussian blue staining showing intense accumulation of FAD USPIO (as blue stain) in vascular structures. Triple fluorescence images of muscle sections after FAD USPIO injection did not show a significant accumulation of FAD USPIO inside the vessels (E–G), which was co-validated using Prussian blue staining. On Prussian blue-stained images of LnCap tumors from the control group ($n = 4$), hardly any accumulation of Resovist could be detected and also no fluorescence could be seen in the 530 nm channel. Together, these observations clearly show that FAD USPIO mostly accumulate in angiogenic tumor endothelium. (For interpretation of the references to colour in this figure legend, the reader is referred to the web version of this article.)

accumulation is more related to an RCP-mediated uptake than to unspecific phagocytosis by RES-associated cells. This finding was supported by preliminary *in vivo* MR competitive binding experiments demonstrating reduced FAD USPIO uptake after addition of 10-fold free FAD (own unpublished observations).

3.6. Immunofluorescence and Prussian blue staining

Immunofluorescence analyses and Prussian blue staining of tumor and muscle cryosections were performed to validate the MR findings. Tumor and muscle vessels were stained using a primary rat anti-mouse CD31 (PECAM-1) endothelial cell marker antibody in combination with a Cy3-labeled anti-rat IgG secondary antibody (red) and nuclei were counterstained with DAPI (blue). Triple fluorescence images of the LnCap tumor sections showed an intense co-localization of the FAD USPIO probe (green) (Fig. 4A and C) with the endothelial cell markerCD-31 (red) (Fig. 4B and C). Contrarily, triple fluorescence images of muscle sections showed no evident FAD USPIO accumulation (Fig. 4E–G) also not in the mature and stable vasculature. In agreement with these observations, Prussian blue staining was performed, which clearly showed the accumulation of FAD USPIO inside the tumor, compared to almost no accumulation in muscle as shown in Fig. 4D and H, respectively. In contrast, Prussian blue images of tumors of the Resovist-treated control mice hardly showed any accumulation of Resovist (Fig. 4L). As expected, only very little amounts of FAD USPIO and Resovist were found in the extravascular compartment and inside tumor cells.

4. Conclusions

In summary, adsorptive FAD coating of USPIO renders them highly specific for RCP, leading to an intense uptake by prostate cancer and activated angiogenic endothelial cells. FAD USPIO display intense fluorescence, stability under physiological conditions and exhibit an MR contrast enhancement similar to Resovist. Additionally, after intravenous injection FAD USPIO intensely accumulate in the endothelial cell compartment of prostate cancer xenografts, which could be assessed with 3T MRI and by immunofluorescence microscopy. Thus, these results suggest that FAD USPIO can serve as a valid tool for *in vivo* molecular MR imaging of the metabolism of angiogenic vessels in tumors and thus as an indirect marker of tumor angiogenesis. As a follow up study, based on flavins such as FMN or FAD small molecular optical imaging (OI) and PET probes will be generated to gain better extravasation and to pave the way for enhanced tumor cell targeting. Up to now, hardly any data is available on the regulation of RCP in healthy tissues. Using molecular imaging probes as suggested in this article may further help to evaluate the suitability of RCP as an imaging biomarker of tumor and tissue metabolism.

Acknowledgments

This work was supported by the DFG grant KI 1072/1-3 “Dual modal contrast agents for MRI and Optical Imaging techniques” by the InnoMeT grant z0909im008a “Entwicklung und Bildgebung patientenoptimierter Implantate”. The authors would like to thank Dr. P. Müller (RWTH Aachen University) for powder XRD measurements.

Appendix A. Supplementary data

Supplementary data related to this article can be found at http://dx.doi.org/10.1016/j.biomaterials.2012.08.036.

References

[1] Mason CW, D'Souza VM, Bareford LM, Phelps MA, Ray A, Swaan PW. Recognition, co-internalization, and recycling of an avian riboflavin carrier protein in human placental trophoblasts. J Pharmacol Exp Ther 2006;317(2):465–72.

[2] Kirkpatrick ND, Zou C, Brewer MA, Brands WR, Drezek RA, Utzinger U. Endogenous fluorescence spectroscopy of cell suspensions for chemopreventive drug monitoring. Photochem Photobiol 2005;81(1):125–34.

[3] Ostrander JH, McMahon CM, Lem S, Millon SR, Brown JQ, Seewaldt VL, et al. Optical redox ratio differentiates breast cancer cell lines based on estrogen receptor status. Cancer Res 2010;70(11):4759–66.

[4] Mujat C, Greiner C, Baldwin A, Levitt JM, Tian F, Stucenski LA, et al. Endogenous optical biomarkers of normal and human papillomavirus immortalized epithelial cells. Int J Cancer 2008;122(2):363–71.

[5] Skala MC, Riching KM, Gendron-Fitzpatrick A, Eickhoff J, Eliceiri KW, White JG, et al. In vivo multiphoton microscopy of NADH and FAD redox states, fluorescence lifetimes, and cellular morphology in precancerous epithelia. Proc Natl Acad Sci USA 2007;104(49):19494–9.

[6] Foraker AB, Khantwal CM, Swaan PW. Current perspectives on the cellular uptake and trafficking of riboflavin. Adv Drug Deliv Rev 2003;55(11):1467–83.

[7] Huang SN, Swaan PW. Involvement of a receptor-mediated component in cellular translocation of riboflavin. J Pharmacol Exp Ther 2000;294(1):117–25.

[8] Huang SN, Phelps MA, Swaan PW. Involvement of endocytic organelles in the subcellular trafficking and localization of riboflavin. J Pharmacol Exp Ther 2003;306(2):681–7.

[9] Karande AA, Sridhar L, Gopinath KS, Adiga PR. Riboflavin carrier protein: a serum and tissue marker for breast carcinoma. Int J Cancer 2001;95(5):277–81.

[10] Johnson T, Ouhtit A, Gaur R, Fernando A, Schwarzenberger P, Su J, et al. Biochemical characterization of riboflavin carrier protein (RCP) in prostate cancer. Front Biosci 2009;14:3634–40.

[11] Bareford LM, Phelps MA, Foraker AB, Swaan PW. Intracellular processing of riboflavin in human breast cancer cells. Mol Pharmacol 2008;5(5):839–48.

[12] Holladay SR, Yang Z, Kennedy MD, Leamon CP, Lee RJ, Jayamani M, et al. Riboflavin-mediated delivery of a macromolecule into cultured human cells. Biochim Biophys Acta 1999;1426(1):195–204.

[13] Plantinga A, Witte A, Li MH, Harmon A, Choi SK, Banaszak Holl MM, et al. Bioanalytical screening of riboflavin antagonists for targeted drug delivery—a thermodynamic and kinetic study. ACS Med Chem Lett 2011;2(5):363–7.

[14] Thomas TP, Choi SK, Li MH, Kotlyar A, Baker Jr JR. Design of riboflavin-presenting PAMAM dendrimers as a new nanoplatform for cancer-targeted delivery. Bioorg Med Chem Lett 2010;20(17):5191–4.

[15] Witte AB, Timmer CM, Gam JJ, Choi SK, Banaszak Holl MM, Orr BG, et al. Biophysical characterization of a riboflavin-conjugated dendrimer platform for targeted drug delivery. Biomacromolecules 2012;13(2):507–16.

[16] Roming M, Luensdorf H, Dittmar KEJ, Feldmann C. ZrO(HPO(4))(1-x)(FMN)(x): quick and easy synthesis of a nanoscale luminescent biomarker. Angew Chem Int Ed Engl 2010;49(3):632–7.

[17] Jayapaul J, Hodenius M, Arns S, Lederle W, Lammers T, Comba P, et al. FMN-coated fluorescent iron oxide nanoparticles for RCP-mediated targeting and labeling of metabolically active cancer and endothelial cells. Biomaterials 2011;32(25):5863–71.

[18] Yu FX, Goh SR, Dai RP, Luo Y. Adenosine-containing molecules amplify glucose signaling and enhance Txnip expression. Mol Endocrinol 2009;23(6):932–42.

[19] Bumb A, Brechbiel MW, Choyke PL, Fugger L, Eggeman A, Prabhakaran D, et al. Synthesis and characterization of ultra-small superparamagnetic iron oxide nanoparticles thinly coated with silica. Nanotechnology 2008;19(33):335601.

[20] Jander G, Jahr K. Massanalyse. 17 ed; 2009. p. 219–21.

[21] Bashir WA. Photometric determination of iron (III). Microchem J 1981;26(4):477–80.

[22] Umekita Y, Hiipakka RA, Kokontis JM, Liao S. Human prostate tumor growth in athymic mice: inhibition by androgens and stimulation by finasteride. Proc Natl Acad Sci U S A 1996;93(21):11802–7.

[23] Chowdhury MH, Lakowicz JR, Ray K. Ensemble and single molecule studies on the use of metallic nanostructures to enhance the intrinsic emission of enzyme cofactors. J Phys Chem C Nanomater Interfaces 2011;115(15):7298–308.

[24] Becvar J, Palmer G. The binding of flavin derivatives to the riboflavin-binding protein of egg white. A kinetic and thermodynamic study. J Biol Chem 1982;257(10):5607–17.

[25] Ruoslahti E, Bhatia SN, Sailor MJ. Targeting of drugs and nanoparticles to tumors. J Cell Biol 2010;188(6):759–68.

[26] Reimer P, Balzer T. Ferucarbotran (Resovist): a new clinically approved RES-specific contrast agent for contrast-enhanced MRI of the liver: properties, clinical development, and applications. Eur Radiol 2003;13(6):1266–76.